Development and Performance Estimates of a Ducted Tandem CRP

Masaju Igeta*, Hongbin Yuan
Niigata power systems Co., Ltd.
125-1, Nishishinmachi, Ohta-city, Gunma, 373-0847, Japan
*masaju_igeta@niigata-power.com

ABSTRACT

In recent years, with the rising in oil price, marine propulsors are being demanded as higher efficiency. Consequently, a ducted CRP (i.e. Contra-Rotating Propeller; hereinafter referred to as the device), which was expected to provide an improved efficiency, was developed by Niigata Power Systems Co. Ltd.

The device is a tandem CRP with a duct (a Kort nozzle) set up in aft propeller. Comparing to a single propeller in high loading, the device could increase an effect of the duct thrust due to the flow entering aft ducted propeller has been accelerated by fore propeller. As a CRP with these characteristics, the device is considered suitable for domestic vessels operating in low-speed, high loading conditions.

The water tank tests were carried out parametrically with sorted by the sizes of two propellers, the gaps and the power ratios (or revolution ratios) between the fore and aft propellers, to verify the device's characteristics mentioned above. These tests results indicated that an increased efficiency could be achieved. Additionally, a CFD (Computational Fluid Dynamics) investigation was performed to analyze the interaction between the both propellers and a likely improvement in hydrodynamic performance was found. These results are presented.

Keywords

ducted CRP, internal flow, hydrodynamic performance

1. INTRODUCTION

Lowered fuel oil consumption, reduced vessel vibration and noise, increased bollard pull and propulsion efficiency, and high maneuverability, can all be derived from the beneficial effects of improved hydrodynamic performance. It is, therefore, not surprising that the classic problem of high efficiency and compact propulsion system design are being recognized as an important element for competitive ship operating under harsh conditions, e.g. tugboat, multi-purpose and other domestic vessels.

With regard to such the purpose, a ducted tandem Contra-Rotating Propellers (CRP) was developed by Niigata Power Systems. The design philosophy is based on CRP and ducted propeller being both classified as high efficiency propulsors. For the CRP, due to both propellers, which rotate in counter directions, can lead to the swirl flow that leaves the fore propeller partly is recovered. CRP is torque-balanced, which provides better stability and accurate positioning to vessels. In the case of ducted azimuth thruster, the accelerating flow type of nozzle can offer an increasing in efficiency for heavily loaded propeller due to its airfoil nozzle; with horizontal rotating throughout 360°, azimuth thruster controls the thrust direction (steering) instead of the rudder. These beneficial features are very significant for a domestic vessel operating in low-speed, high loading conditions and with a compact construction.

Replacing conventional propeller with an aft ducted azimuth thruster, the present CRP combines with fore propeller after a ducted azimuth thruster as shown in figure 1, the schematic of the ducted tandem CRP system equipped in ship hull.

For the initial step in development of the ducted CRP, the present work deals with a water tank investigation on hydrodynamic performance parametrically for various conditions in propeller's size, axial gap and power ratio between the two propellers. These test results indicated that there is a higher efficiency for the ducted CRP comparing to a single propeller at thrust loading coefficient Ct=2.5. Furthermore, a viscous numerical analysis was performed to analyze the internal flow around the ducted CRP. Based on the understanding of experimental data and numerical results; a possible improvement for higher efficiency was achieved by modifying the pitch ratio of the aft propeller and giving an appropriate power ratio numerically. These results of performance estimates of the present ducted tandem CRP are described in this paper.

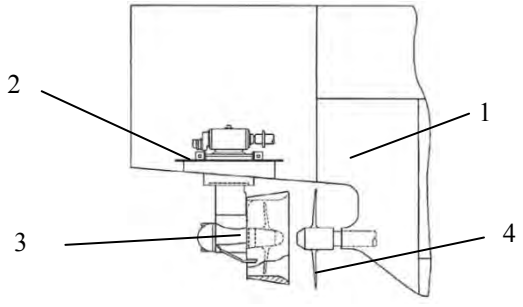

1. Ship Hull
2. Hydraulic Steering Unit
3. Ducted Azimuth Thruster
4. Fore Propeller

Fig.1 schematic of ducted tandem CRP equipped in ship

2. EXPERIMENTAL MEASUREMENTS

2.1 Test Apparatus and CRP Models

Figure 2 shows the test model of ducted CRP combining a fore open propeller and an aft ducted propeller coaxially. For ducted propeller, the geometric composition of the ducted and propeller affects performance significantly. Ideal position was designed in consideration of thrust efficiency. The characteristics of the two propellers were shown in table 1 and the cross-section of duct model is shown in figure 3.

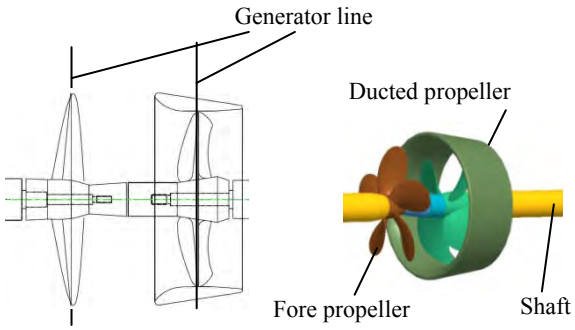

Fig. 2 configuration of the ducted CRP test

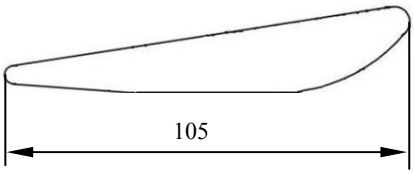

Fig. 3 19A nozzle

Table 1 Configuration characteristics of the test propeller

Position	Fore	Aft
Diameter (mm)	210, 245, 255, 300	210
Pitch Ratio	0.7	1.000
E.A.R	0.65	0.65
Boss Ratio	0.18	0.23
Rake	0	0
Number of Blade	5	4
Blade Section	MAU	Skewed Kaplan

The model water test was carried out by using the cavitation tunnel. Fore propeller dynamometer and aft propeller dynamometer installed in the upstream and downstream flow of the ducted CRP respectively were employed for measuring thrust and torque of the two propellers. The 19A nozzle was attached in bottom of the tunnel through the strut and fearing. Fluid force which acts on a nozzle was measured through a Six-component balance. Figure 4 shows the closed-up schematic of the cavitation tunnel and measuring detectors.

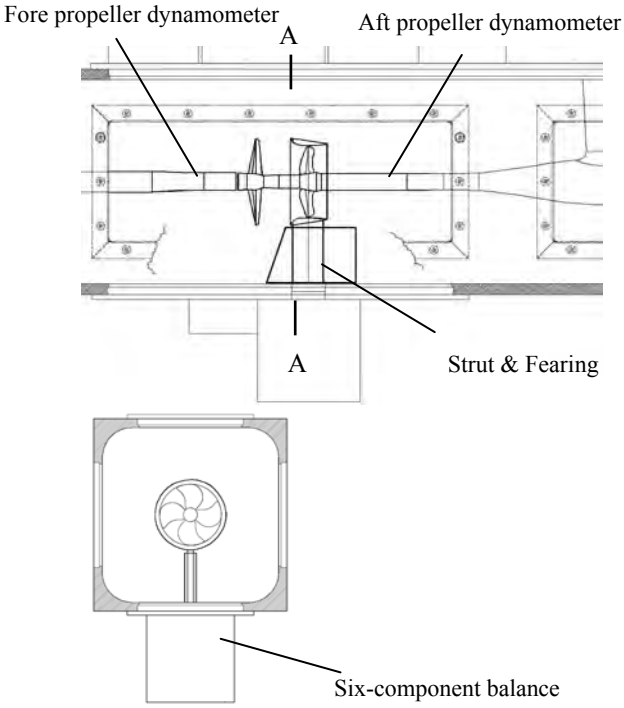

Fig.4 cavitation tunnel test apparatus and measuring detectors

The water tank tests discussed in this paper involve three parametrical conditions varying in loading ratio, diameter ratio and axial gap between the fore and aft propeller. Each test was carried out to investigate the effect on propeller performance at advance ratio J_F=0.4. J_F is the advance ratio of the fore propeller and calculated as the following:

$$J_F = \frac{V_{inlet}}{N_F Df} \qquad (1)$$

Where V_{inlet} = uniform inflow; Df = diameter of the fore propeller; N_F= revolution of the fore propeller.

The 5 couples of loading ratio between the fore propeller and aft propeller were defined in 7:3, 6:4, 5:5, 4:6 and 3:7 for evaluating the effects of loading ratio. For the investigation of the effects of propeller diameter, the fore propeller diameter was changed in accordance with the characteristic list of the present test model (table1), ranged in diameter from ϕ 210 to ϕ 300mm. Three axial gaps between two propellers in 0.8Df, 0.6Df and 0.45Df were employed for testing and discussing the effects of the propeller axial gap.

The results of efficiency were used for comparing with the results of a single propeller in order to evaluate the propeller performance of the ducted CRP. The propeller performance was estimated by calculating the efficiency η_0 given in the formula (2).

$$\eta_0 = \frac{J_F K_{Ttotal}}{2\pi K_{Qtotal}} \qquad (2)$$

Where K_{Ttotal}= total thrust coefficient; K_{Qtotal}= total torque coefficient. Both the two coefficients were evaluated based on the diameter of the fore propeller *Df*, and the two revolutions of the fore propeller and aft propeller. The K_{Ttotal} and K_{Qtotal} were calculated by the formulas (3) and (4), respectively.

$$K_{Ttotal} = \frac{T_F + T_{AP} + T_D}{\rho N_F^{\ 2} Df^{\ 4}} \qquad (3)$$

$$K_{Qtotal} = \frac{Q_F + Q_A \frac{N_A}{N_F}}{\rho N_F^{\ 2} Df^{\ 5}} \qquad (4)$$

Where T_F = thrust of the fore propeller; T_{AP} = thrust of the aft propeller; T_{AD} = thrust of the duct; N_F = revolution of the fore propeller; the thrust of the fore propeller, N_A=revolution of the aft propeller.

2.2 Test Results

The performance characteristics of CRP model in efficiencies with respect to thrust loading coefficients *Ct* were shown in figure 5, 6 and 7 for loading ratio, propeller diameter and axial gap, respectively. In general, for a propulsor operating in domestic vessels, the propeller performances are evaluated typically at the thrust loading coefficient *Ct* 2.5. *Ct* is defined by the following formula.

$$C_t = \frac{8K_{Ttotal}}{\pi J_F^{\ 2}} \qquad (5)$$

In figure 5, the single propeller was more efficient than the ducted CRP at low thrust loading coefficient. It was about 2 point high in efficiency for the single propeller to compare to the ducted CRP at the highest efficiency. However, at the high loading coefficient, the ducted CRP shows the higher efficiency comparing to the single propeller. These comparisons indicated the tendency that the ducted CRP can obtain a high efficiency with the loading coefficient increasing.

Concerning the influence of power ratio between two propellers, the power ratio was determined to 5:5 for the cases of the changing in Propeller diameter and propeller axial gap.

With a fore propeller in ϕ 210mm diameter, the ducted CRP was improved about 1 point increase in efficiency at *Ct* 2.5, comparing to the conventional single propeller as shown in figure 6.

For the different propeller axial gaps, the case of the 0.6*Df* axial gap indicated the lowest efficiency among the three axial gaps at *Ct* 2.5 and few noticeable improvements in efficiency were observe as shown in figure 7.

Based on the above results, the ducted CRP with the same diameter at ϕ 210mm for two propellers, same power ratio at 5:5, 0.6*Df* axial gap and 1 point increase in efficiency at *Ct* = 2.5, was considered as the most efficient among the test models. This model was employed for investigating the hydrodynamic phenomena in detailed numerically.

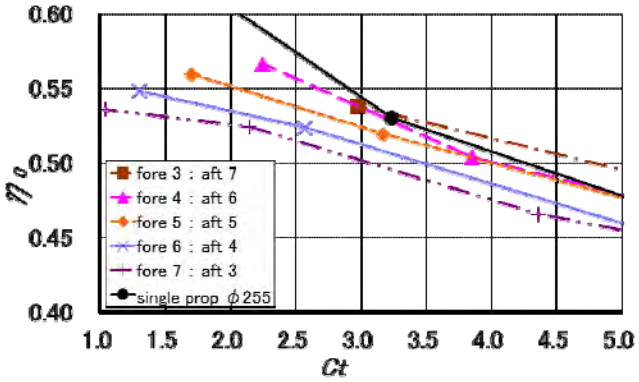

Fig.5 comparisons of efficiencies at different loading ratios

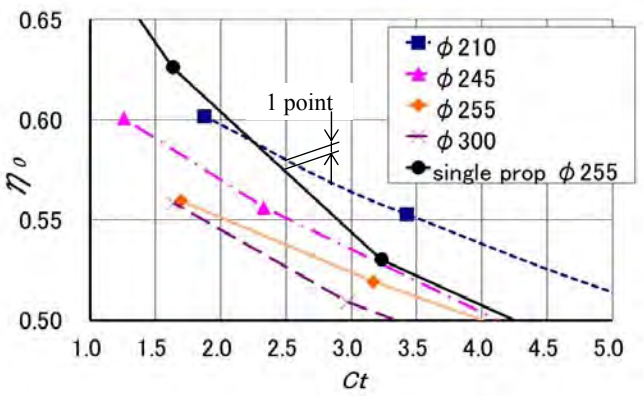

Fig.6 comparisons of efficiencies at different propeller diameters

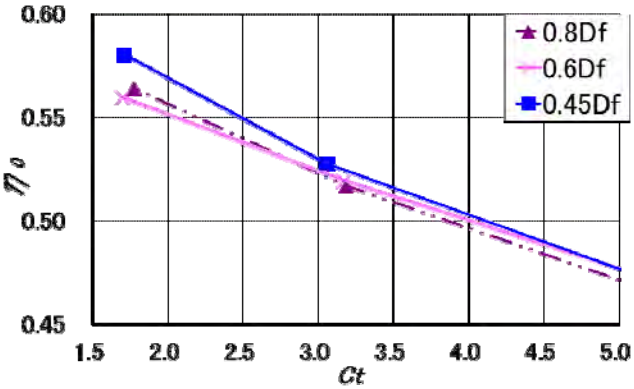

Fig.7 comparisons of efficiencies at different axial gaps

3. NUMERCIAL METHODOLOGY

Numerical simulation was performed in order to enhance the understanding of the entire flow field around the ducted CRP. The Several viscous numerical analyses of the flow field in marine propeller, focusing on the propeller wake behavior and propeller blade tip vortex flow, were reported by Uto et al. (1992, 1993), Stanire et al (1998) and Rhee et al. (2005). Based on these validated results, a three-dimensional, steady-state, Reynolds Averaged Navier-Stokes (RANS) equations coupled with the realizable k-ε turbulence model was solved for

investigating on hydrodynamic performance and internal flow of the present ducted CRP.

Concerning the domain discretization, the RANS code used a cell-centered, finite-volume method that allows the use of computational cells of arbitrary polyhedral mesh in order to enable a more accurate geometry modeling.

3.1 Calculation Domain and Grid System

Figure 8 shows calculation domain around the CRP. The cylindrical domain was generated with structured and unstructured multi-block grid with 8Df in diameter and 8.6Df in axial length. In order to accurately resolve the viscous wakes, the meshes around the two propellers were particularly treated with 641,595 cells and 373,373 cells for the fore and aft propeller, respectively. Grid dependency is examined by varying grid density in the blocks, revealing that the total cell 2,557,253 for the calculation domain was finally determined by comparing the numerical results to experimental ones.

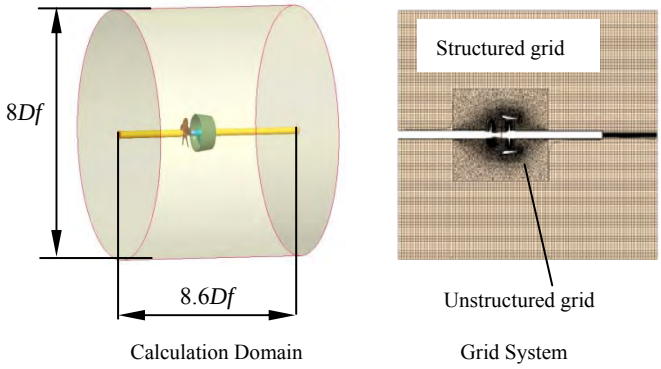

Fig. 8 calculation domain and grid system

3.2 Definition of the Reference Frame

Figure 9 shows the two opposite rotating regions for the two propellers. The duct and the domain extension upstream and downstream of the two propellers were assumed to be in the stationary frame of reference, whereas the grid blocks surrounding the two propellers were in the rotating frame of reference. Thus, three interfaces were created at the junction among three different reference frames. Applying for a steady-state simulation, two interfaces models are available. The mixing-plane between two different reference frames performs inflow and outflow boundary conditions for one pitch passage of the fore and aft propeller by circumferential averaging process. This major drawback found that the averaging scheme could produce a nonphysical mixing loss at interface, Denton (1990) whereas applying "Frozen Rotor" model the wake/core profile was preserved across the interface and was found to be useful in identifying the internal flow structures. The major drawback of "Frozen Rotor" model is the different relative positions resulting in different solutions. This problem could be overcome by performing an unsteady-state calculation to obtain a more accurate time-averaged solution.

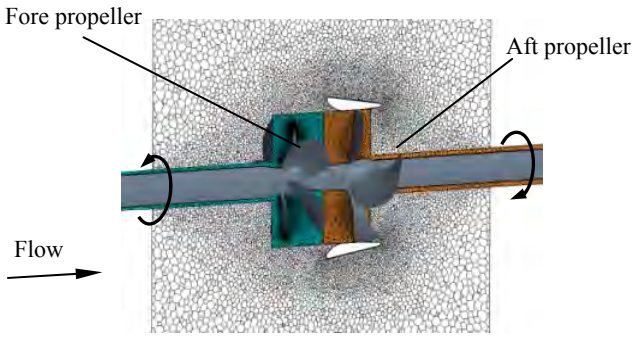

Fig. 9 two opposite-rotating regions of the two propellers

4. RESULTS AND DISCUSSIONS

4.1 Validation with Experimental Data

The numerical results for the various advance ratios were validated with experimental data. The non-dimensional values, total thrust coefficient K_{Ttotal}, total torque coefficient K_{Qtotal} and efficiency coefficient η_0 were used to evaluate the propeller performance of the present CRP. The comparisons of propeller performance between experiments and CFD were plotted in figure 10.

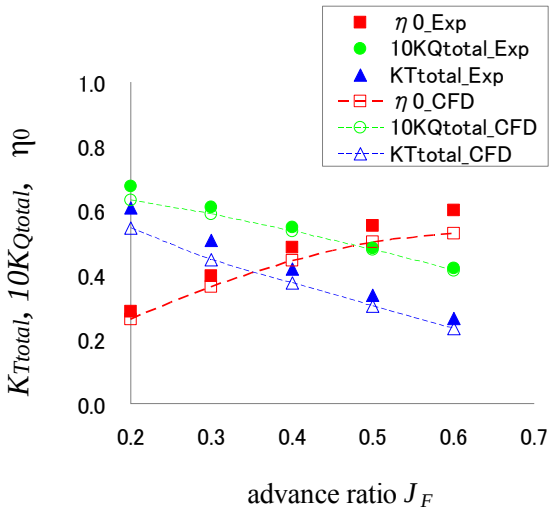

Fig. 10 comparisons of propeller performance results between test and CFD at J_F= 0.2-0.6

As shown in figure 10, a largely good agreement between the results of the numerical simulation and the test are presented, except for the values of thrust and torque at low advance ratios at J_F=0.2-0.3 being lightly under-predicted. To these moments, the authors have not come up with a completed explanation for these discrepancies. The possible reasons are followed that the RANS failed to predict the appearance of the transition on the blade suction side, probably due to its intense numerical viscosity, and over-predicted efficiency of the propeller caused by non-uniformed inflow affected by the tunnel wall experimentally.

4.2 Internal Flow in Ducted CRP

Concerning the hydrodynamic performance of the CRP, the total velocity which includes the inflow, the interactions between two propellers and the induced velocities of two propellers, was evaluated for the ducted CRP. The investigating cross-sections were located

upstream and downstream of the CRP along the rotational axis X_i at three advance ratios J_F=0.2, 0.4, 0.6. The fore propeller located at axial position X_1=0 while the aft propeller at X_2=0.6*Df*. The various locations of the velocity planes for the fore and aft propellers were shown in figure 11. The circumferentially averaged velocities in axial component at a given radial location 0.7*R* of each cross-section were shown in figure 12, where *R* is propeller radius. For each advance ratio, the axial velocity changed smoothly with respect to non-dimension allocation, X_i/0.6*Df*, the more large gradients took place around the fore propeller than did at the aft propeller. An approximate in axial velocity is observed near the leading edge of the aft propeller at each advance ratio J_F, these equivalent velocities occurred at the location X_i/0.6*Df* >0.75. Especially, The increased inflow (the axial velocity) of the aft propeller indicated that it is possible for the aft propeller to be optimized by changing the its pitch based on the propeller characteristics.

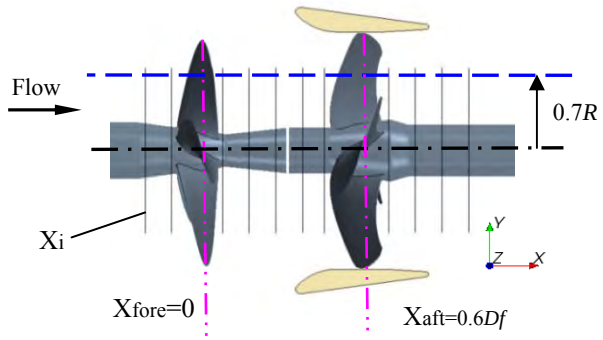

Fig. 11 locations of the velocity planes for the fore and aft propellers

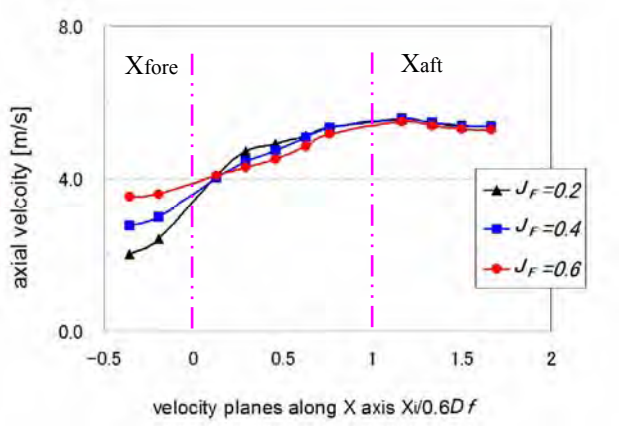

Fig.12 axial velocity distributions along the X axis at advance ratio J_F=0.2, 0.4, 0.6

The propeller wake plays a crucial role in ship wake signature and a propulsor design concerning the propulsion effect. Figure 13(b) presents the comparisons of the circumferentially averaged velocity in axial (V_a), tangential (V_t) and radial (V_r) component for the two cross-sections located in X_1=0.54*Df* and X_2=1.5*Df* of the ducted CRP (figure 13(a)) at J_F=0.4. The velocities distributed along the spanwise of propeller blade at dimensionless radius r/R=0.29, 0.44, 0.59, 0.74, 0.90 and 1.05, where *r* is radial position and *R* is propeller radius.

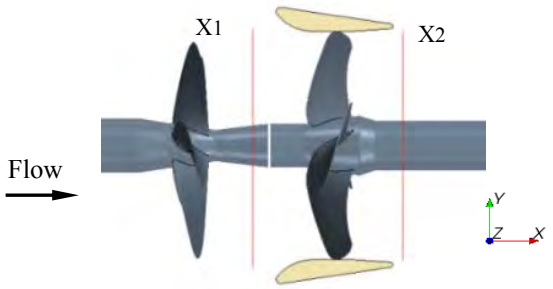

Fig. 13(a) the section location along X axis at X1, X2

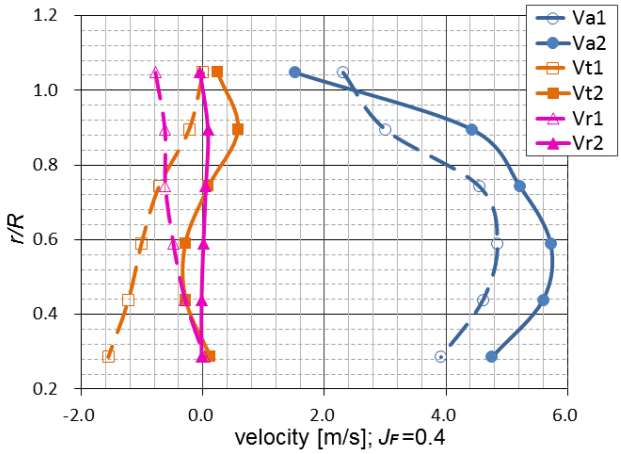

Fig. 13(b) Comparisons of averaged velocities for two section locations shown in Fig.13 (a) at J_F=0.4

As shown in figure 13 (b), for the section location X_2 axial velocity V_{a2} component was accelerated, and the radial velocity V_{r2} and tangential velocity V_{t2} components were reduced comparing to the each velocity component , V_{a1}, V_{r1} and V_{t1} of the cross-section X_1. The decrease of the radial velocity indicated that the duct was quite effective to prevent the growth of the spanwise flow of the aft propeller. For the wake of the fore propeller, there is the lower tangential velocity component around the propeller hub at X_2 comparing to the one at X_1. For the wake of the aft propeller, the opposite swirl flow occurred at the region where the radius of the propeller is larger than 0.7*R*. To this phenomena, the velocity vector on the two locations are clearly shown in figure 14. Obviously, the opposite swirl flow was generated by the aft propeller. The residues of the swirl flow at the ducted CRP outflow X_2 indicated that the design of the present ducted CRP was not so successful.

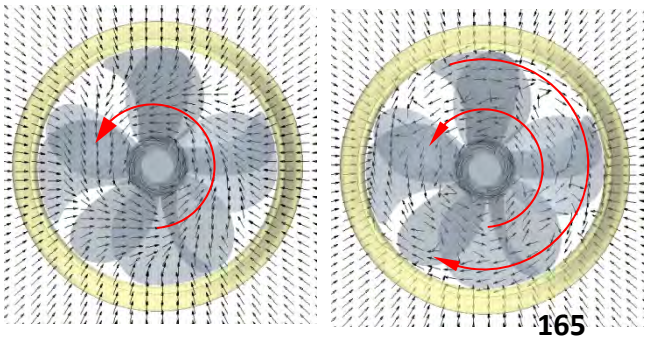

Fig. 14 velocity vectors for two section locations at X1(left) and X2(right) shown in Fig.13 (a) at J_F=0.4

4.3 Effect of Changing Pitch Ratio of the Aft Propeller

Based on the validated numerical method and the understanding of the experimental and numerical results shown previously, the efficiency in case of varying the geometry parameters relating with the fore and aft propeller and the duct could be explored by using the present numerical method. Kirihata et al. (1991) investigated engine performance and propeller efficiency of the ship with controllable pitch propeller and concluded the propeller efficiency increased with increment of propeller pitch angle in remarkable inclination under the condition of low ship speed. For the present work, an extension in pitch ratio to 1.2 for the aft propeller was investigated in order to predict a possible improvement of propeller characteristics.

To estimate propulsion performance in a given power ratio (i.e.5:5 at J_F=0.4), the present numerical methodology enabled the authors to settle the power ratio by coordinating the revolutions of the fore and aft propeller separately. Figure 15 presents the comparison of efficiencies among the improved CRP, the primary test CRP and the single propeller. The comparing results indicated that there is an efficiency gain close to 2.5 point for the improved CRP comparing to the single propeller at *Ct*=2.5.

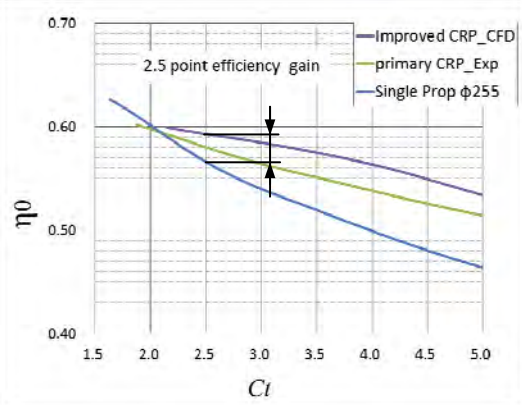

Fig.15 Comparison of efficiencies among the improved CRP, primary test CRP, and the single propeller at *Ct*=2.5

5. CONCLUDING REMARKS

The propulsion performance of the ducted tandem CRP was investigated experimentally and numerically. The numerical results were found to agree satisfactorily with available experimental data.The present work suggested as follows.

1. The water tank test indicated that the ducted CRP at two propellers in same diameter ϕ 210mm and 0.6*Df* propellers' gap can produce about 1 point increase in efficiency comparing to the conventional single propeller under the same thrust loading *Ct*=2.5.

   It is significant for the ducted tandem CRP to be able to operate in regions where the draft is being limited and don't desire a larger diameter of propeller, such as the operating of domestic vessels. The improvement of the hydrodynamic performance verified a good concept on the ducted CRP in design.
2. Few noticeable improvements in propeller efficiency were observed by varying the gaps between two propellers.
3. With the rising in power ratio of the aft propeller to the fore propeller, the efficiency of the ducted CRP indicated an inclination to increase.
4. The numerical results indicated that the presence of duct induced the decrease in radial velocity component of the aft propeller. It can conclude that an energy saving was contributed by the duct.
5. Extending the pitch ratio of the aft propeller with a matched power ratio between the two propellers, 2.5 point of efficiency gain was obtained by using the present numerical method. It is effective for this present method to provide a prediction on propeller performance as the first step of development.

6. FUTURE WORK

The authors are planning to conduct more investigation on hydrodynamic performance of ducted CRP affected by the considerable geometry condition such as propeller blade and duct shape, and the more detailed flow structures in ducted CRP under unsteady state numerically and experimentally.

7. ACKNOWLEDGMENT

The authors are grateful for the cooperation in water tank test from IHI Co. Japan.

REFERENCES

Shin Hyung RHEE and Shitalkumar JOSHI (2005), "Computational Validation for Flow around a Marine Propeller Using Unstructured Mesh Based Navier-Stokes Solver", JSME International Journal.

Uto,S., (1992), "Computation of Incompressible Viscous Flow around a Marine Propeller," J. Soc. Naval Architects of Japan, 172, PP.213-224.

Uto,S., (1993), "Computation of Incompressible Viscous Flow around a Marine Propeller, 2nd Report: Turbulent Flow Simulation," J. Soc. Naval Architects of Japan, 173, PP.67-75.

Oh, K.-J., and Kang, S.-H., 1995, "Numerical Calculation of the Viscous Flow around a Propeller Shaft Configuration," Int. J. for numerical Methods in Fluids, 21(1), pp.1-13.

Stanier, M., (1998), "The Application of 'RANS' Code to Investigate Propeller Scale Effects," Proc. 22nd Symposium on Naval Hydrodynamics, Washington, DC.

Denton, J.D., (1990), "The Calculation of Three Dimensional Viscous Flow Through Multistage Turbomachines", ASME 90GT-19.

Tomoaki Kirihata et al. (1991), “Studies on Engine Performance and Propeller Efficiency of the Ship with Controllable Pitch propeller”(Japanese), The Journal of Shimonoseki University of Fisheries, Japan.